Coupled Dielectric Nanoparticles Manipulating Metamaterials Optical Characteristics

Shabnam Ghadarghadr, *Student Member, IEEE*, and Hossein Mosallaei, *Senior Member, IEEE*

***Abstract*—In this paper, we investigate the concept and theory of all-dielectric metapatterned structures that manipulate electric and magnetic optical characteristics. A 3-D array of dielectric particles is designed, where the spheres operate in their magnetic modes and their couplings offer electric modes. An analytical solution for the problem of plane wave scattering by 3-D array of dielectric nanospheres is presented. FW multipole expansion method is applied to express the optical fields in terms of the electric and magnetic dipole modes and the higher order moments. By enforcing the boundary conditions at the surface of each sphere, with the use of the translational addition theorem for vector spherical wave functions, required equations to determine the scattering coefficients are obtained. Novel materials features in optics are demonstrated. Electric and magnetic scattering coefficient resonances around the same frequency band are obtained. It is highlighted how a metapatterned structure constructed from dielectric nanosphere unit cells can provide electric and magnetic modes resulting in backward wave phenomenon. A comprehensive circuit model based on RLC (resistor, inductor, and capacitor) realization is presented to successfully analyze the scattering performance of a dielectric nanosphere. To better understand the physics of an array of spheres, circuit models for the interactions, and couplings between spheres are also accomplished. The engineered dispersion diagram for a 3-D array of identical highly coupled nanospheres is scrutinized, verifying that the high couplings between spheres can offer the backward wave characteristics.**

***Index Terms*—Array of nanospheres, backward wave behavior, dielectric metamaterial, electric resonance, engineered dispersion diagram, magnetic resonance, metapatterned structure, nanometamaterial.**

I. Introduction

INTERESTS in artificial optical materials are increasing in the scientific communities [1]–[3]. During the last few years, there have been considerable efforts to develop metamaterials in RF/microwave frequencies; however, this progress has not been as rapid as expected in the optical domain. The goal of this paper is to theoretically demonstrate the optical performance of arrays of dielectric nanoparticles enabling coupled electric and magnetic mode features.

To achieve an optical material with the functionality of interest, one needs to create appropriate electric and magnetic dipole modes in a building block unit cell [4], [5]. Essentially, the electric and magnetic dipole moments are the basic foundations for making metamaterials, and novel arrangements of these dipole moments can lead to the desired material properties. Recently, a unique paradigm for metamaterial evolvement was introduced by Holloway *et al.* [6], where they designed a double negative (DNG) metamaterial by embedding an array of magnetodielectric spherical particles in a background matrix. The work of Holloway *et al.* is based on the mixing formulas obtained by Lewin [7]. Later on Vendik *et al.* proposed a more practical approach by utilizing only dielectric particles, where they arranged two different dielectric spheres in one unit cell, such that one sphere generates electric dipole mode while the other establishes magnetic dipole mode [8]. Combining these two features, one can provide a metamaterial with both (ϵ, μ) effective parameters (above the resonant frequencies, negative constitutive permittivity and permeability parameters are obtained [4]). However, the low dielectric material of the nanospheres in optical regimes generates some difficulties in tuning the terahatz (THz) DNG medium, if two sets of nanospheres are used. In this study, we use one set of dielectric nanoparticles to accomplish the backward wave behavior in THz spectrum.

Over the past few years, there has been much improvement in the fabrication, design, and modeling of nanostructures [9]. Most of the current modeling techniques of nanostructures are based on the discrete dipole approximation (DDA), finite-difference time domain (FDTD), finite-element method (FEM), and T-matrix [10]–[16]. Numerical methods can be extremely accurate and comprehensive, but they are somehow time-consuming. Theoretical approaches have the great advantage of providing fast solutions, where they can illustrate the physics and concept of nanostructures at the same time. As an example of efficient techniques, Alam *et al.* [17], [18] investigated an accurate analytical method based on the circuit model analogy to calculate the resonance frequency and scattering parameters of a single plasmonic particle. Hanson *et al.* [19] suggested another efficient approach for obtaining the electromagnetic interactions between a carbon nanotube and an electrically small plasmonic sphere (where the sphere is characterized by its dipole moment). The focus of this paper is to apply an analytical method based on the electric and magnetic dipole modes to characterize the performance of a 3-D array of dielectric nanoparticles and understand their unique physical features. The characteristic equations and electric and magnetic resonant phenomena for the nanostructures are derived. An intuitive circuit analogy is also exploited to obtain a better understanding of the resonant behavior of the array of spheres.

Manuscript received August 15, 2008; revised November 25, 2008. First published January 20, 2009; current version published September 4, 2009. This work was supported in part by the US National Science Foundation (NSF). The review of this paper was arranged by Associate Editor J. Rogers.

The authors are with the Electromagnetics and Optical Meta-Devices Laboratory, Electrical and Computer Engineering Department, Northeastern University, Boston, MA 02115 USA (e-mail: shabnamg@ece.neu.edu; hosseinm@ece.neu.edu).

Color versions of one or more of the figures in this paper are available online at http://ieeexplore.ieee.org.

Digital Object Identifier 10.1109/TNANO.2009.2013619

The 3-D array of gallium phosphide (GaP) particles is tailored to establish backward wave phenomena. The objective is to create electric and magnetic dipole modes by utilizing 3-D array of nanospheres. Hence, the problem of multiple scattering of a plane wave by an array (either finite or infinite) of dielectric spheres is solved, with the use of multipole expansion method and the translational addition theorem for the vector spherical wave functions [20]–[22]. It is shown that if the particles are small enough or the frequency is such that the magnitudes of higher order modes are negligible compared to dipole modes, dipole modes give accurate descriptions of the traveling waves in the array. We illustrate that by bringing the dielectric spheres close to each other, the couplings between them are increased such that both electric and magnetic resonances can be achieved around the same frequency region.

Accurate closed-form solutions for the scattering coefficients are obtained by utilizing *RLC* (resistor, inductor, and capacitor) circuit modeling. The developed model intuitively describes the physics of the scattering coefficients, and their dependence on the material properties and the array configuration. The proposed circuit model is based on the theoretical derivations and confirmed by comparing it with the exact solutions.

Dispersion diagram characteristics for an array of dielectric spheres are also attained and backward wave performance is explored. It is highlighted how a metamaterial constructed from identical nanospheres has the potential to provide a medium with coupled electric and magnetic dipole moments. The formulations and results presented in this paper will be of great importance for characterizing all-dielectric metamaterial nanostructures.

II. Single-Sphere Electric and Magnetic Dipole Modes

In this section, we highlight the concept of electric and magnetic dipoles creation by using dielectric spheres. To achieve a functional optical metamaterial with desired parameters, it is required to first create the appropriate electric and magnetic dipole moments and then tailor them to the applications of interest. The electric and magnetic dipoles are envisioned as the alphabet for making new structures [5].

To provide a physical insight of dipole mode creation by using dielectric particles, let us begin with the problem of a plane wave and a dielectric sphere centered at (r_p, θ_p, ϕ_p). We assume that a sphere with radius a and dielectric constant ϵ_r is embedded in free space (in general, it can be any other background matrix). A plane wave excitation with the propagation vector $\mathbf{k}$ that lies in the xz plane with harmonic time dependence $\exp(j\omega t)$ is assumed. The electric field is considered to be y-polarized. The incoming incident field on the sphere can be expanded in terms of spherical wave vectors of the first kind $\mathbf{M}^{(1)}_{mn}$ and $\mathbf{N}^{(1)}{}_{mn}$ [20]

$$\mathbf{E}^i_p = \sum_{n=1}^{\infty}\sum_{m=-n}^{n}\left[A^{ip}_{mn}\mathbf{N}^{(1)}_{mn}(r_p,\theta_p,\phi_p) + B^{ip}_{mn}\mathbf{M}^{(1)}_{mn}(r_p,\theta_p,\phi_p)\right] \quad (1a)$$

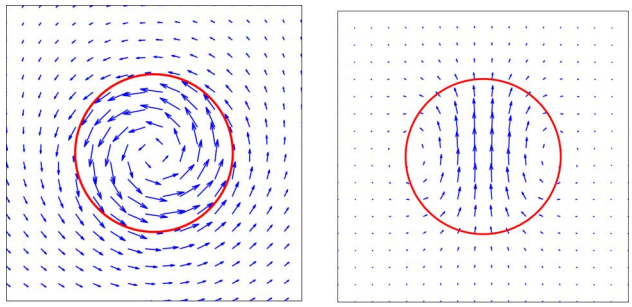

(a) (b)

Fig. 1. Vector spherical wave functions field lines. (a) $\mathbf{M}_1$ field lines. (b) $\mathbf{N}_1$ field lines.

$$\eta\mathbf{H}^i_p = -j\sum_{n=1}^{\infty}\sum_{m=-n}^{n}\left[A^{ip}_{mn}\mathbf{M}^{(1)}_{mn}(r_p,\theta_p,\phi_p) + B^{ip}_{mn}\mathbf{N}^{(1)}_{mn}(r_p,\theta_p,\phi_p)\right] \quad (1b)$$

where η is the free space intrinsic impedance and the incident-field expansion coefficients are derived in [23]. For the special case of end-fire incidence, we have [24]

$$A^{ip} = B^{ip} = \frac{-1}{j^n}\frac{2n+1}{n(n+1)}\delta_{m,1}e^{-j\mathbf{k}.\mathbf{r}_p}. \quad (2)$$

Following the same routine, the scattered field can be represented as a weighted sum of spherical wave vector of the third kind $\mathbf{M}^{(3)}_{mn}$ and $\mathbf{N}^{(3)}_{mn}$. A^{sp}_{mn} and B^{sp}_{mn} are considered the unknown scattered coefficients to be obtained by matching the boundary conditions at the surface of the nanosphere. Note that $\mathbf{M}^{(1)}_{mn}(\mathbf{M}^{(3)}_{mn})$ and $\mathbf{N}^{(1)}_{mn}(\mathbf{N}^{(3)}_{mn})$ are the spherical vector wave functions representing the incoming (outgoing) waves associated with spherical Bessel (Hankel) functions.

It must be recalled that spherical vector wave function $\mathbf{M}$ has the circular field lines, that is to say, the radial components of all $\mathbf{M}$ functions are zero. Hence, if only the A^{sp}_{mn} coefficients are excited, the field has a radial component of $\mathbf{E}(\mathbf{E} \propto \mathbf{N})$, where the magnetic field is always perpendicular to the radial vector $(\mathbf{H} \propto \mathbf{M})$. In other words, the distribution of electromagnetic (EM) or optical fields is such as it would be produced by electric charges on the surface of the sphere. Therefore, A^{sp}_{mn} can be envisioned as electric scattered coefficients [24]. If, on the other hand, only B^{sp}_{mn} are excited, the field is such as would be produced by oscillating magnetic charges on the surface of the sphere and the field is said to be of magnetic type. Hence, B^{sp}_{mn} are the magnetic scattered coefficient [24]. The field lines for $\mathbf{M}_{11}$ and $\mathbf{N}_{11}$ are shown in Fig. 1. Manifestly, the near-field pattern of $\mathbf{M}_{11}$ is very similar to the electric field pattern of a magnetic dipole, while the near-field pattern of $\mathbf{N}_{11}$ resembles to the electric field pattern of an electric dipole. Hence, if only A^{sp}_{11} is excited, the nanosphere is equivalent to an electric dipole moment, where if only B^{sp}_{11} exists, the nanosphere reveals the behavior of a magnetic dipole.

Note that the quantities in (1) are defined with respect to a local spherical coordinate system. Forcing the boundary

conditions at the surface of the nanosphere directs us to

$$A_{mn}^{sp} = \varsigma_n(a) A_{mn}^{ip} \tag{3a}$$

$$B_{mn}^{sp} = \xi_n(a) B_{mn}^{ip} \tag{3b}$$

where $\varsigma_n(a)$ and $\xi_n(a)$ are the normalized Mie electric and magnetic scattering coefficients for a single dielectric sphere [21], [24]. The scattering coefficients are very important in any application that involves the creation and use of electric and magnetic moments. Their resonances are the principal parameters for manipulating the performance of a nanosphere. The formal mathematical solutions for these scattering coefficients are known for years; however, the physics of these parameters may not be grasped efficiently. It is then important to develop a model that can easily explain the physical features of these coefficients [25]. In the next section, we present a circuit model to successfully tailor the scattering coefficients. This idea was initially proposed by Alam *et al.* [18], where they used *RLC* circuit realization for modeling the scattering coefficients of a plasmonic nanosphere.

A. RLC Modeling

Due to the nature of spherical Bessel functions and their derivatives, Mie's solutions in its present form may not be suitable to characterize the physics of the problem. Expressing the scattering coefficients in terms of polynomial continued fractions helps to effectively elucidate the optical scattering and resonance properties of a nanostructure. Here, we present an accurate circuit model based on the *RLC* realization for the scattering coefficients of a single dielectric sphere in the optical spectrum. Basically, we reduce the scattering problem to a circuit type problem. Note that the scattering coefficients are in fact the input impedance of the circuit model. Let us first expressed the scattering coefficients as

$$\varsigma_n(a) = -\frac{1}{1 - jX_E(n, ka, \epsilon_r)} \tag{4a}$$

$$\xi_n(a) = -\frac{1}{1 - jX_H(n, ka, \epsilon_r)} \tag{4b}$$

where X_E and X_H are

$$X_E(n, ka, \epsilon_r) = \frac{y_n(ka)(k_p a j_n(k_p a))' - \epsilon_r j_n(k_p a)(k a y_n(ka))'}{j_n(ka)(k_p a j_n(k_p a))' - \epsilon_r j_n(k_p a)(k a j_n(ka))'} \tag{5a}$$

$$X_H(n, ka, \epsilon_r) = \frac{j_n(k_p a)(k a y_n(ka))' - y_n(ka)(k_p a j_n(k_p a))'}{j_n(k_p a)(k a j_n(ka))' - j_n(ka)(k_p a j_n(k_p a))'} \tag{5b}$$

j_n and y_n are the spherical Bessel and Neumann functions, respectively. Without loss of generality, in this paper, we only investigate the circuit models for the first electric and magnetic scattering coefficients. In order to derive an accurate simple model for the coefficients, the spherical Bessel and Neumann functions are evaluated by using the rational function expansions [26]. Since higher order terms contribute negligible values to the scattering coefficients, we only keep the terms with order of eight or less (for $ka < 1$). If we define $x = ka$ and $m = \sqrt{\epsilon_r}$, we end up with, as shown (6a) and (6b), at the bottom of this page, where

$$a_1 = \frac{4m^2(35m^4 + 405m^2 + 819)}{-13m^4(5m^2 + 36)} \tag{7a}$$

$$a_2 = \frac{216(m^6 + 20m^4 + 49m^2 - 70)}{13m^4(5m^2 + 36)} \tag{7b}$$

$$a_3 = \frac{6048(m^4 + 9m^2 - 10)}{-13m^4(5m^2 + 36)} \tag{7c}$$

$$a_4 = \frac{60480(m^2 + 2)}{13m^4(5m^2 + 36)} \tag{7d}$$

$$e_1 = -\frac{20(m^2 - 1)}{(m^4 - 6m^2 + 5)} \tag{7e}$$

$$e_2 = \frac{120}{(m^4 - 6m^2 + 5)}. \tag{7f}$$

For simplicity, we refer to the denominator coefficients of (6a) and (6b) as $b_1 - b_2$ and f_1. To derive explicit *RLC* models, the rational functions given by (6) are expanded as continued fraction forms of polynomial terms. Hence, the scattering coefficients are achieved as the input impedances of *RLC* ladder types circuits (see also Fig. 2)

$$\varsigma_1(a) = -\frac{1}{1 + jX_{1e} + 1/(jX_{2e} + (1/jX_{3e}))} \tag{8a}$$

$$\xi_1(a) = -\frac{1}{1 + jX_{1h} + (1/jX_{2h})} \tag{8b}$$

$$X_E(1, x, m) \approx \left(\frac{65}{144x^3}\right)\left(\frac{m^2(5m^2 + 36)}{5m^4 + 13m^2 - 13}\right) \times \frac{x^8 + a_1 x^6 + a_2 x^4 + a_3 x^2 + a_4}{x^4 - (105840(m^4 - 1)/756m^2(5m^4 + 13m^2 - 13))x^2 + (1058400(m^2 - 1)/756m^2(5m^4 + 13m^2 - 13))} \tag{6a}$$

$$X_H(1, x, m) \approx -\frac{21(m^4 - 6m^2 + 5)}{4m^4 x^5} \times \frac{x^4 + e_1 x^2 + e_2}{x^2 - (14(m^2 - 1)/m^4)} \tag{6b}$$

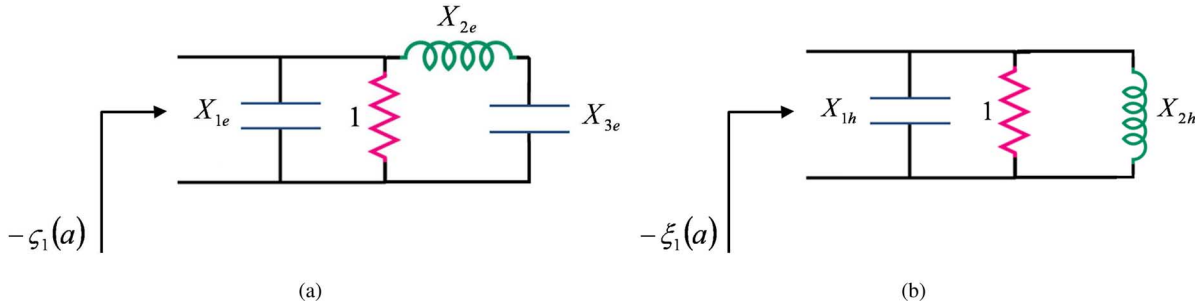

Fig. 2. *RLC* schematics for Mie scattering coefficients. (a) Electric scattering coefficient. (b) Magnetic scattering coefficient.

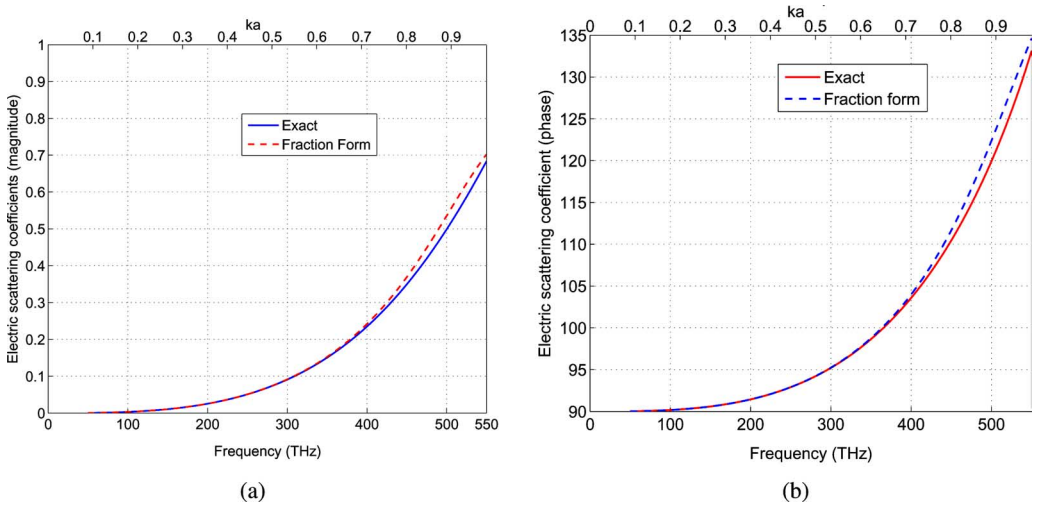

Fig. 3. Electric scattering coefficients for a single GaP sphere of radius $a = 85$ nm and $\epsilon_r = 12.25$. Comparison between *RLC* ladder type model versus exact Mie solution. (a) Magnitude. (b) phase.

where

$$X_{1e} = \frac{65}{144x^3}\frac{m^2(5m^2+36)}{5m^4+13m^2-13} \times \left(x^4+(a_1-b_1)x^2+a_2+b_1^2-b_2-a_1b_1\right) \quad (9a)$$

$$X_{2e} = \frac{65}{144x^3}\frac{m^2(5m^2+36)}{5m^4+13m^2-13}\left(\frac{x^2}{c_1}+\frac{b_1c_1-c_2}{c_1^2}\right) \quad (9b)$$

$$X_{3e} = \frac{65}{144x^3}\frac{m^2(5m^2+36)}{5m^4+13m^2-13}(c_1x^2+c_2) \times \left(\frac{-c_1}{b_1c_2}+\frac{1}{b_2}+\frac{c_1^2}{c_2^2}\right) \quad (9c)$$

$$X_{1h} = -\frac{21(m^4-6m^2+5)}{4m^4x^5}(x^2+(e_1-f_1)) \quad (9d)$$

$$X_{2h} = -\frac{21(m^4-6m^2+5)}{4m^4x^5}\frac{x^2+f_1}{f_1^2+e_2-e_1f_1} \quad (9e)$$

and

$$c_1 = a_1(b_1^2-b_2)-a_2b_1+a_3-b_1(b_1^2-2b_2) \quad (10a)$$

$$c_2 = a_1b_1b_2-a_2b_2+a_4-(b_1^2-b_2)b_2. \quad (10b)$$

It is worth mentioning that $X_{1e}-X_{3e}$ and $X_{1h}-X_{2h}$ denote the reactance parts of the scattering coefficients. Depending on the material property (m) and frequency, they can be either inductive or capacitive. Note that if $mka \gg 1$ and $ka > 1$, these approximations might not be valid.

B. Simulation Results

To evaluate the accuracy of our approach, we compare the results of RLC technique with the exact Mie solutions. For a nano-GaP sphere with $\epsilon_r = 12.25$ and radius of 85 nm, the normalized Mie scattering coefficients are depicted in Figs. 3 and 4. As it is illustrated, there is a negligible difference between the RLC modeling and the exact Mie solutions, indicating that our circuit model can properly predict the behavior of the scattering coefficients for a dielectric sphere. Note that in this scenario, ka is between 0 and 1, and m is as high as $\sqrt{12.25}$. It is worth highlighting that these circuit models are obtained only for the first electric and magnetic scattering coefficients.

The capability of representing the scattering coefficients with RLC circuit models allows one to apply the well-known concepts in circuit theory to effectively design required elements for providing desired electric and magnetic resonances.

It is interesting to mention that Figs. 3 and 4 show that at the magnetic resonance ($f = 485$ THz), $A_{11}^{sp} < \frac{1}{2}B_{11}^{sp}$ or $\varsigma_1(a) < \frac{1}{2}\xi_1(a)$, namely at the resonance of the magnetic scattering coefficient, the nanosphere behaves mostly as a magnetic dipole

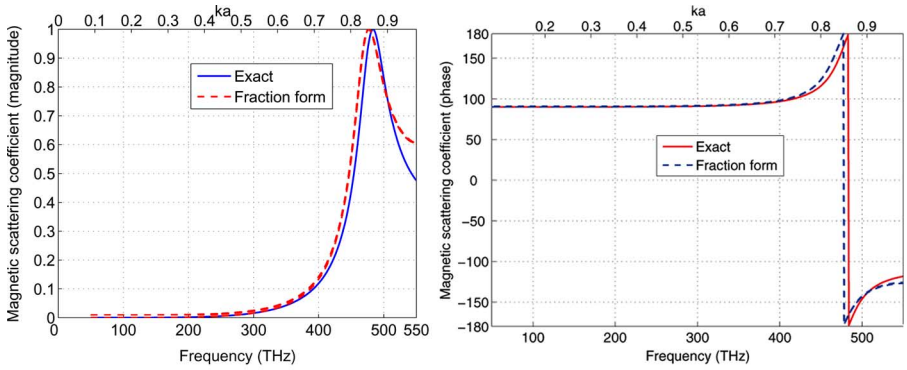

(a) (b)

Fig. 4. Magnetic scattering coefficients for a single GaP sphere of radius $a = 85$ nm and $\epsilon_r = 12.25$. Comparison between *RLC* ladder type model versus exact Mie solution. (a) Magnitude. (b) phase.

$(\mathbf{E} \propto \mathbf{M})$, where the coupling between low-dielectric spheres has increased electric scattering co-efficient. The same argument can be done for the electric resonance at $f = 643$ THz (however, here the plots are demonstrated only in the frequency spectrum of interest). In summary, the dielectric nanospheres can provide electric and magnetic dipole moments at the electric and magnetic resonances of the scattering coefficients. Novel combinations of these modes can offer desired metamaterial features.

III. Meta Patterned Array of Dielectric Nanospheres

A 3-D array of spheres has the potential to manipulate the coefficients of $\mathbf{M}$ and $\mathbf{N}$ in a novel fashion that the metamaterial with functionality of interest can be achieved. In this section, we develop the required formulations for characterizing the performance of a 3-D array of dielectric spheres. Full-wave electric and magnetic multipole couplings are considered for the performance modeling. The problem of multiple scattering is solved by matching the boundary conditions at the surfaces of all spheres. To impose the boundary conditions at the surface of each sphere (the reference sphere), the local coordinates of other spheres are translated to the local coordinate of the reference sphere using the additional translation theorem for vector spherical wave functions [22], [23]. By utilizing these, the desired system of linear equations for the scattering coefficients is achieved. We also obtain the engineered dispersion relation for an infinite 3-D array of dielectric spheres by generalizing this concept. Moreover, we demonstrate RLC circuit theory to model the interactions and couplings between spheres. Modern nanomaterial performances are also highlighted.

A. Modeling and Analysis

The geometry of the 3-D array of nanospheres is depicted in Fig. 5. Each nanosphere is represented with dielectric constant of ϵ_r and radius a. The spheres are centered at $x = l_x h_x, y = l_y h_y$, and $z = l_z d$, where $l_x = \pm 1, \pm 2, \pm 3, \ldots \pm L_x, l_y = \pm 1, \pm 2, \pm 3, \ldots \pm L_y$, and $l_z = 0, 1, 2, \ldots, L_z$.

The goal is to determine the scattering coefficients for every sphere by forcing the boundary conditions at the surface

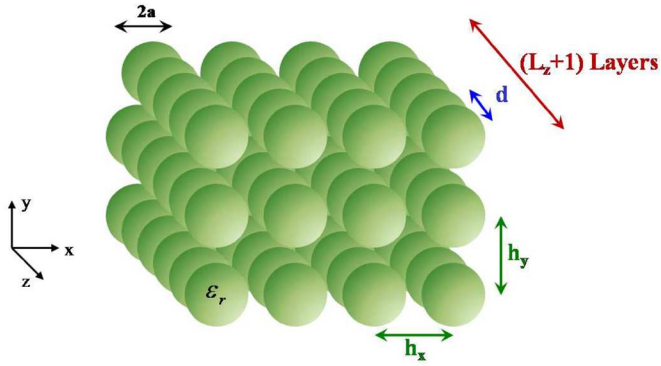

Fig. 5. Configuration of an array of dielectric nanospheres.

of that particle. To implement the boundary conditions at the surface of each sphere (e.g., pth sphere), the outgoing scattered fields from all other spheres are expressed in the local coordinate of the reference sphere (pth sphere). The continuity of the tangential electric and magnetic fields is applied by using the spherical vector translational addition theorem [22]. The solution for the unknown scattering coefficients is then obtained as [23]

$$A_{mn}^{sp} = \varsigma_n(a)\left(A_{mn}^{ip} + \sum_{\substack{q \\ q\neq p}} \sum_{\nu=1}^{\infty} \sum_{\mu=-\nu}^{\nu} \left[A_{mn}^{\mu\nu}(d_{pq}, \theta_{pq}, \phi_{pq}) A_{\mu\nu}^{sq} + B_{mn}^{\mu\nu}(d_{pq}, \theta_{pq}, \phi_{pq}) B_{\mu\nu}^{sq}\right]\right) \tag{11a}$$

$$B_{mn}^{sp} = \xi_n(a)\left(B_{mn}^{ip} + \sum_{\substack{q \\ q\neq p}} \sum_{\nu=1}^{\infty} \sum_{\mu=-\nu}^{\nu} \left[A_{mn}^{\mu\nu}(d_{pq}, \theta_{pq}, \phi_{pq}) B_{\mu\nu}^{sq} + B_{mn}^{\mu\nu}(d_{pq}, \theta_{pq}, \phi_{pq}) A_{\mu\nu}^{sq}\right]\right). \tag{11b}$$

where the summation over q is the summation on all nanoparticles except the reference sphere, d_{pq} is the center distance between the pth nanosphere and the qth one [23]. $A_{mn}^{\mu\nu}$ and

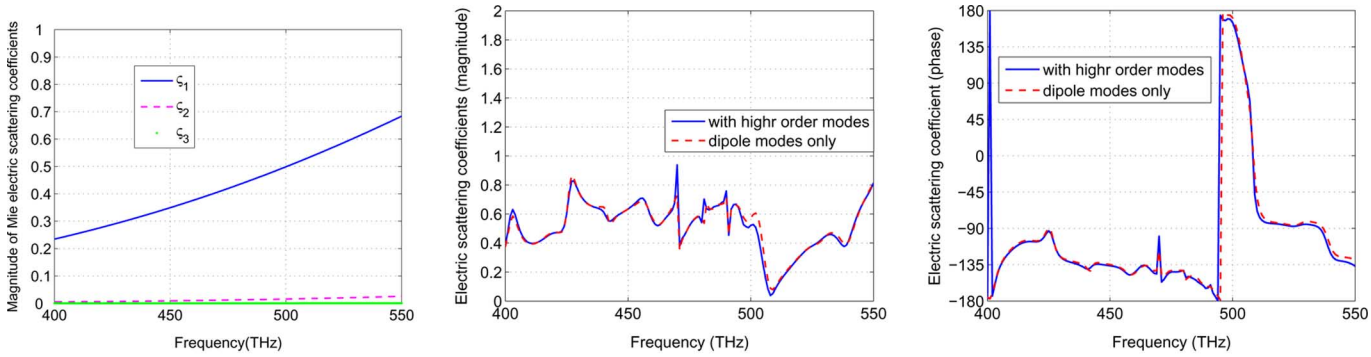

(a) (b) (c)

Fig. 6. Electric scattering coefficients for a GaP nanosphere with $\epsilon_r = 12.25$ and $a = 85$ nm. (a) Normalized Mie scattering coefficient for the first three terms. The performance of electric scattering coefficient for a sphere inside a finite array with $L_x = 4$, $L_y = 4$, $L_z = 2$, and unit cell size of $d/a = 2.23$ and $h_x = h_y = 2.1a$. (b) Magnitude. (c) Phase.

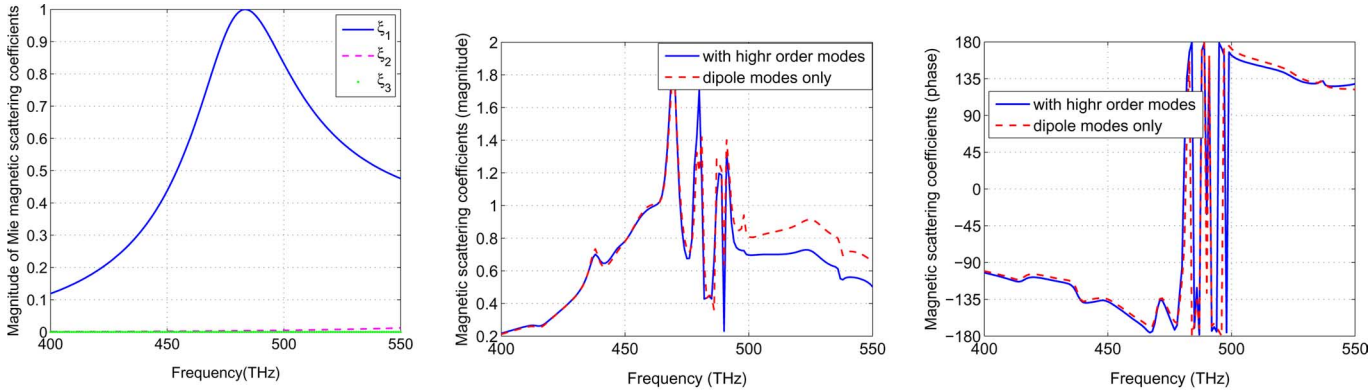

(a) (b) (c)

Fig. 7. Magnetic scattering coefficients for a GaP nanosphere with $\epsilon_r = 12.25$ and $a = 85$ nm. (a) Normalized Mie scattering coefficient for the first three terms. The performance of magnetic scattering coefficient for a sphere inside a finite array with $L_x = 4$, $L_y = 4$, $L_z = 2$, and unit cell size of $d/a = 2.23$ and $h_x = h_y = 2.1a$. (b) Magnitude. (c) Phase.

$B_{mn}^{\mu\nu}$ are the translational addition theorem coefficients given in [22]. Equations (11) are a coupled set of complex linear algebraic equations, and should be solved simultaneously to yield the unknown scattering coefficients. In addition, the infinite series must be truncated to a finite number $n = \nu = N$ and $m = \mu = M$.

If the spheres are small enough or the frequency is such that the magnitude of higher order modes are negligible compared to the magnitude of the first electric and magnetic modes, only the dipole scattered fields are excited. And thus the scattered coefficients can be well approximated by only considering $n = 1$. To verify this idea, we analyze the performance of the scattered coefficients for an array of dielectric nanospheres with radius of $a = 85$ nm, $\epsilon_r = 12.25$, $L_x = L_y = 4$, and $L_z = 2$. A plane, wave excitation having a y-polarized electric field that propagates in the z-direction is assumed. The results are described in Figs. 6 and 7. As it is shown in the frequency bands where $\varsigma_n(a), \xi_n(a)|_{n>1} \ll \varsigma_1(a), \xi_1(a)$, one can assume that only the first electric and magnetic dipole modes are excited. It is worth noting that Figs. 6 and 7 depict the electric and magnetic scattered coefficients for a sphere located in the middle of the array ($l_x = l_y = 0, l_z = 1$). In the followings, we assume that either the spheres are sufficiently small or the frequency is such that the spheres' scattering can be treated with only dipole vector spherical waves.

We now address the potential applications of electric and magnetic dipoles for developing novel metamaterials by tailoring their scattering coefficients. As illustrated earlier, based on the Mie series, dielectric spheres can offer electric and magnetic dipole moments and higher order modes. To obtain a backward wave behavior, one should create the electric and magnetic dipole resonances around the same frequency regime. Here, we investigate the feasibility of making an array of identical dielectric spheres for nanometamaterial development. Spheres operate in their magnetic resonant modes, and by increasing their couplings, electric modes are created. Hybrid modes (combination of electric and magnetic dipole moments) will manipulate a metapatterned structure with the desired figures of merit.

The scattered coefficients are the key parameters that dictate the performance of the dielectric resonator. Therefore, to generate the backward wave metamaterial behavior using one set of dielectric spheres, one should tune the resonances of the electric scattering coefficients to occur at the resonances of the magnetic scattering coefficients. For a sphere inside an array,

the characteristic frequencies are derived solving (11), thus, by changing the array configuration, one can achieve the electric and magnetic resonances around the same frequency region.

To show how the array formation can control the performance of the electric and magnetic resonances, we consider a periodic array of dielectric nanospheres. The array is taken to be infinite in the x- and y-directions ($L_x = L_y = \infty$) and finite in the z-direction. The plane wave incident on the array is set to be y-polarized with the z- directed propagation vector $\mathbf{k}$. Since we are exploring the traveling waves supported by the periodic array of spheres, the spheres' scattering coefficients in a layer are identical. Hence, we have a linear system of $2(L_z+1)$ equations to be solved for the electric and magnetic scattered coefficients. For $l \in \{0, 1, \ldots, L_z\}$, we obtain (the frequency is considered such that only the first dipole modes can be excited)

$$[\Lambda]\begin{bmatrix}[A_{11}^{sl}]\\ [B_{11}^{sl}]\end{bmatrix} = \begin{bmatrix}[\varsigma_1(a)A_{11}^{il}]\\ [\xi_1 a B_{11}^{il}]\end{bmatrix} \tag{12}$$

where

$$[\Lambda] = \begin{bmatrix}\overline{\overline{I}} - [\varsigma_1(a)\Sigma_{ll_z}] & -[\varsigma_1(a)\Sigma'_{ll_z}]\\ -[\xi_1(a)\Sigma'_{ll_z}] & \overline{\overline{I}} - [\xi_1(a)\Sigma_{ll_z}]\end{bmatrix} \tag{13a}$$

$$\Sigma_{ll_z} = \sum_{\substack{l_y=-\infty\\(l_x,l_y,l_z)\neq(0,0,l)}}^{\infty}\sum_{l_x=-\infty}^{\infty} h_0^{(2)}(kr) - \frac{1}{2}h_2^{(2)}(kr)P_2(\cos\theta) \tag{13b}$$

$$\Sigma'_{ll_z} = \sum_{\substack{l_y=-\infty\\(l_x,l_y,l_z)\neq(0,0,l)}}^{\infty}\sum_{l_x=-\infty}^{\infty} \frac{-3j}{2}h_1^{(2)}(kr)P_1(\cos\theta) \tag{13c}$$

$$\mathbf{r} = l_x h_x \hat{x} + l_y h_y \hat{y} + (l_z - l)d\hat{z} \tag{13d}$$

where A_{11}^{sl} and B_{11}^{sl} represent the electric and magnetic scattered coefficients for the layer denoted by l and $\overline{\overline{I}}$ is the identity matrix. Solving the earlier matrix equation, the unknown scattering coefficients are achieved. Primarily, Σ_{ll_z} can be envisioned as the interactions between the electric (magnetic) fields of the reference nanosphere [the sphere centered at $(0,0,l)$] with the electric (magnetic) fields of all other spheres. For $l = l_z$, Σ_{ll} (*self interaction*) denotes the interactions between the electric (magnetic) fields of the reference nanosphere with electric (magnetic) fields of all other spheres located at the same plane as the reference sphere (l). In the same manner, Σ'_{ll_z} is the coupling between the magnetic (electric) fields of reference sphere with the electric (magnetic) fields of all other nanospheres. It is worth mentioning that Σ'_{ll} (*self coupling*) is zero because $P_1(\cos\theta)|_{l=l_z} = 0$. Note that if Σ_{ll_z} and Σ'_{ll_z} are zero, then $[\Lambda]$ is simply the identity matrix, meaning that if there is no interaction or coupling between the spheres, the scattering coefficients are determined by Mie equations.

To better understand the physics of the coupling coefficients and their impact on the metamaterial performance, we will investigate the RLC circuit model for these parameters. By implementing the circuit analogy and acceleration techniques [27], [28], the summations defined in (13) can be realized as the input impedances of RLC type circuits. For a cubic unitcell with $d = h_x = h_y$, where $(l \neq l_z)$ we end up with (the schematics of these circuits are depicted in Fig. 8.)

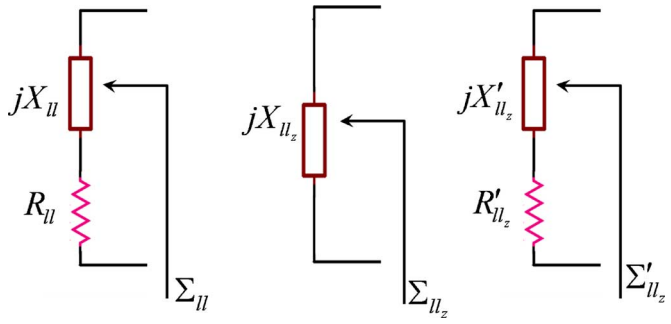

Fig. 8. RLC circuit symbolizing the interactions between spheres $(l \neq l_z)$. Equivalent circuits for Σ_{ll}, Σ_{ll_z}, and Σ'_{ll_z}.

$$\Sigma_{ll} = R_{ll}(kd) + jX_{ll}(kd) \tag{14a}$$

$$\Sigma_{ll_z} = jX_{ll_z}(kd, |l - l_z|) \tag{14b}$$

$$\Sigma'_{ll} = 0 \tag{14c}$$

$$\Sigma'_{ll_z} = R'_{ll_z}(kd, |l - l_z|) + jX'_{ll_z}(kd, |l - l_z|) \tag{14d}$$

where for $0 \leq kd \leq \pi$

$$R_{ll}(kd) \approx \frac{3\pi}{(kd)^2} - 1 \tag{15a}$$

$$R'_{ll_z}(kd, |l - l_z|) \approx \frac{3\pi}{(kd)^2}\cos(|l - l_z|kd) \tag{15b}$$

$$X_{ll}(kd) \approx \frac{3}{4kd}\left[1.2316 + 3\ln\left(\frac{kd}{4\pi}\right) + \frac{1}{6}\left(\frac{2\pi}{kd}\right)^2\right] - \frac{3\ln\left(2\sin(kd/2)\right)}{2kd} + \frac{CL_2(kd)}{(kd)^2} \tag{15c}$$

$$X_{ll_z}(kd, |l - l_z|) \approx -\frac{12\pi}{\sqrt{2}(kd)^3}e^{-|l-l_z|2\pi\sqrt{2}}e^{|l-l_z|\frac{\sqrt{2}(kd)^2}{8\pi}} \tag{15d}$$

$$X'_{ll_z}(kd, |l - l_z|) \approx -\frac{3\pi}{(kd)^2}\sin(|l - l_z|kd) \tag{15e}$$

and $CL_2(kd)$ is the Clausen function of the second kind. Equation (15d) exhibits that X_{ll_z} is always negative. This reveals that the interaction factor (X_{ll_z}) between electric (magnetic) fields of the reference sphere and electric (magnetic) fields of the spheres in other planes (rather than the self plane) are of capacitive type. Also, as can be seen from (15b), (15e), Σ'_{ll_z} has the kind of sinusoidal variation with kd.

For the verification purposes we compare, the exact solutions (13) and the RLC circuit models in Figs. 9 and 10. A very good agreement is observed.

Circuit models presented here allow one to intuitively explain the optical properties of a periodic array of nanospheres. As an instance, for a cubical array of spheres with only one layer in the direction of propagation ($L_z = 0$), the scattering coefficients for

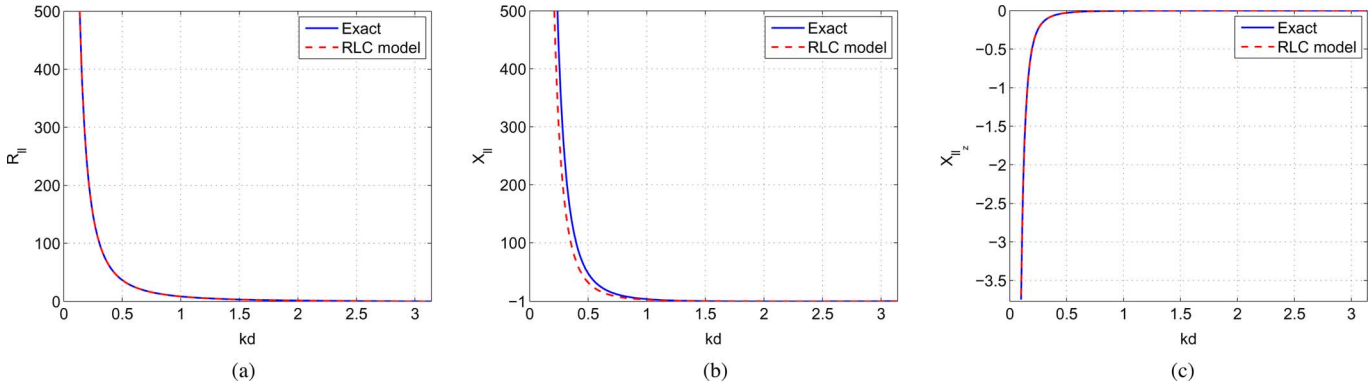

Fig. 9. Performance of the interaction coefficients Σ_{ll_z}. Comparison between the exact solutions and RLC circuit model. (a) $R_{ll}(kd)$. (b) $X_{ll}(kd)$. (c) $X_{ll_z}(kd, 1)$ ($l \neq l_z$).

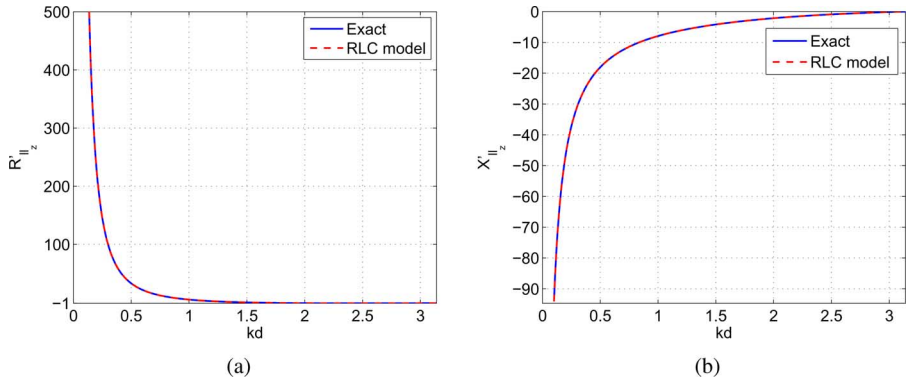

Fig. 10. Performance of the coupling coefficients Σ'_{ll_z}. Comparison between the exact solutions and RLC circuit model ($l \neq l_z$). (a) $R'_{ll_z}(kd, 1)$. (b) $X'_{ll_z}(kd, 1)$.

all spheres are identical (an end-fire incidence is considered)

$$A_{11}^{s1} = \frac{A_{11}^{i1}}{\frac{1}{\varsigma_1(a)} - \Sigma_{00}} = \frac{A_{11}^{i1}}{-\big[1 + R_{00}(kd)\big] + j\big[X_E(1, ka, \epsilon_r) - X_{00}(kd)\big]} \tag{16a}$$

$$B_{11}^{s1} = \frac{B_{11}^{i1}}{\frac{1}{\xi_1(a)} - \Sigma_{00}} = \frac{B_{11}^{i1}}{-\big[1 + R_{00}(kd)\big] + j\big[X_H(1, ka, \epsilon_r) - X_{00}(kd)\big]}. \tag{16b}$$

If the aim is to accomplish both electric and magnetic resonances around the same region, then $X_E = X_{00}$ and $X_H = X_{00}$. In other words, for a specified structure, $X_E(ka)$ should be equal to $X_H(ka)$, which is intrinsically impossible for a dielectric sphere (6). This observation (16) also reveals that to obtain both resonances around the same frequency band, the couplings between electric (magnetic) fields of reference sphere with the magnetic (electric) fields of the other spheres (Σ'_{ll_z}) are also necessitated in addition to the interactions between electric (magnetic) fields of the reference spheres and electric (magnetic) fields of the other spheres.

To better understand the effect of couplings between nanospheres on the scattered coefficients, a three-layer ($L_z = 2$) array of dielectric spheres is investigated. Notice that the eigenfrequencies of the electric and magnetic scattered coefficients are achieved by equating the determinant of the $[\Lambda]$ to zero. Referring to (15d), it can be shown that Σ_{01} and Σ_{02} have small contributions to the determinant of $[\Lambda]$ compared to the other elements. Hence, the characteristic equations (the determinant of $[\Lambda]$) can be well approximated by

$$\Delta_1 = (1 - \varsigma_1(a)\Sigma_{00})(1 - \xi_1(a)\Sigma_{00}) + 2\varsigma_1(a)\xi_1(a)\Sigma'^2_{01} + \varsigma_1(a)\xi_1(a)\Sigma'^2_{02} \tag{17a}$$

$$\Delta_2 = (1 - \varsigma_1(a)\Sigma_{00})(1 - \xi_1(a)\Sigma_{00}). \tag{17b}$$

It is worth mentioning that the resonant frequencies of the nanometamaterial can be predicted from the characteristic equations when $\Delta_1 = 0$ or $\Delta_2 = 0$. Equations (17) are, in fact, the closed-form solutions to characterize the resonance phenomena in nanostructures composed of three layers ($L_x = L_y = \infty$ and $L_z = 2$) of dielectric spheres. These closed-form models help to intuitively explain the scattering behavior of dielectric spheres inside a 3-D array of spheres. In addition to that, the derived closed-form solutions can highlight the dependence of

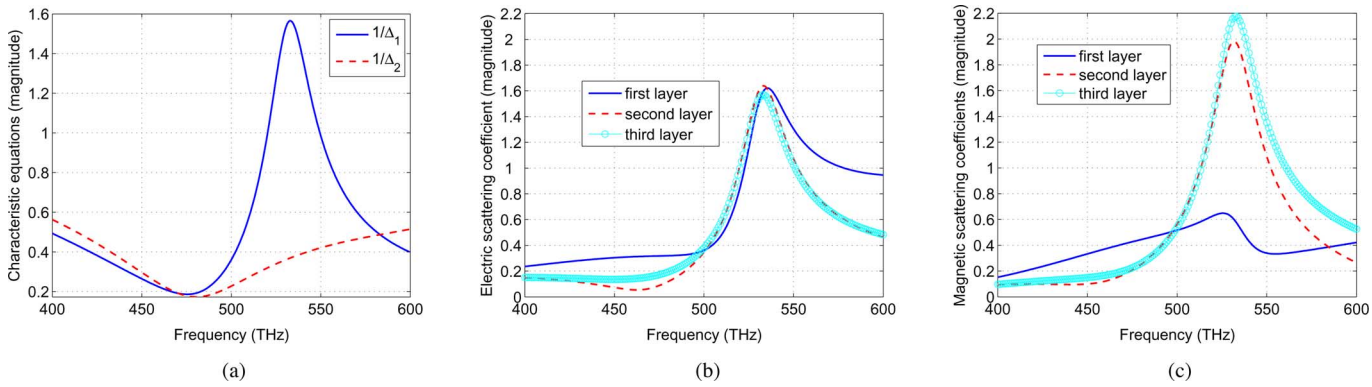

Fig. 11. Performance of a periodic array of GaP nanospheres with three layers in the direction of propagation ($L_z = 2$) and $\epsilon_r = 12.25$, $a = 85$ nm, having unit cell size of $d = 2.23a$ and $h_x = h_y = 2.1a$. (a) Magnitude of $1./\Delta_1$ and $1./\Delta_2$ defined in (17). (b) Electric scattering coefficients (magnitude). (c) Magnetic scattering coefficients (magnitude).

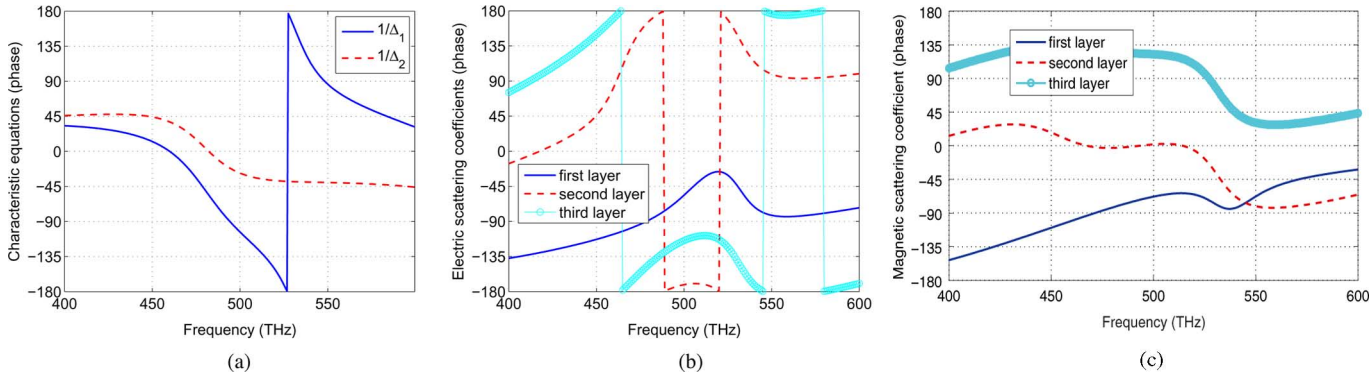

Fig. 12. Performance of a periodic array of GaP nanospheres with three layers in the direction of propagation ($l \neq l_z$) and $\epsilon_r = 12.25$, $a = 85$ nm, having unit cell size of $d = 2.23a$ and $h_x = h_y = 2.1a$. (a) Phases of $1/\Delta_1$ and $1/\Delta_2$ defined in (17). (b) Electric scattering coefficients (phase). (c) Magnetic scattering coefficients (phase).

the resonance behavior on dielectric material, spheres sizes, and the array configuration.

If the intersphere spacings are large enough, then the interactions between spheres ($\Sigma_{00}, \Sigma'_{01}$ and Σ'_{02}) are so small that Λ simplified to the identity matrix, therefore, the eigenfrequencies are accurately described with electric and magnetic resonance frequencies of a single nanosphere defined in (3).

B. Optical Performances of Array of Coupled Spheres

Couplings between the spheres can offer interesting behaviors. Basically, by making the spheres closer to each other, the couplings between them are increased, and can be optimally combined with the magnetic resonances of the spheres causing the electric and magnetic resonances to occur around the same frequency band. To investigate the impact of couplings between spheres, the performance of scattered coefficients for a 3-D array of highly coupled nanospheres is scrutinized. The scattering coefficients for a three-layer array of GaP ($\epsilon_r = 12.5$) nanospheres with radius of $a = 85$ nm, $d/a = 2.23$, and the periodicity of $h_x/a = h_y/a = 2.1$ are depicted in Figs. 11 and 12. As expected, the array configuration manipulate the electric and magnetic scattering coefficients for all layers to have the resonance behavior around the same frequency region. Figs. 11(b) and (c) establish that both electric and magnetic scattering coefficients for all layers resonate around $f = 520$ THz ($\lambda = 576.9$ nm). It is worth mentioning that at this frequency, $a/\lambda = 0.14$, $d/\lambda = 0.33$, and the periodicity in the transverse direction is $h_x/\lambda = h_y/\lambda = 0.31$. The magnitude of $1/\Delta_1$ and $1/\Delta_2$ [characteristic equations defined in (17)] are represented in Fig. 11(a), where it can be seen that, at $f = 520$ THz where electric and magnetic scattering coefficients resonate, Δ_1 tends to zero ($1/\Delta_1$ goes to resonance). From Fig. 11(a), one can observe that, (17a) precisely determines the location of the resonance frequency, which indicates that for a highly coupled array of dielectric spheres, all the interactions and couplings ($\Sigma_{00}, \Sigma'_{01}$ and Σ'_{02}) between one layer and others (including itself) are inevitable. On the other hand, if (17b) anticipates the locations of the resonance frequencies, only interactions between electric (magnetic) fields of each layer with its electric (magnetic) field (*self interaction*) would be taken into the account.

Fig. 12 represents the phase behaviors of the characteristic equations and the scattering coefficients. Fig. 12 (b) and (c) exhibits negative slopes for the phases of scattering coefficients after the resonance, which can be interpreted as a result of backward wave performance. Our simulation results demonstrate that using an array of highly coupled nanospheres, one can achieve backward wave characteristics.

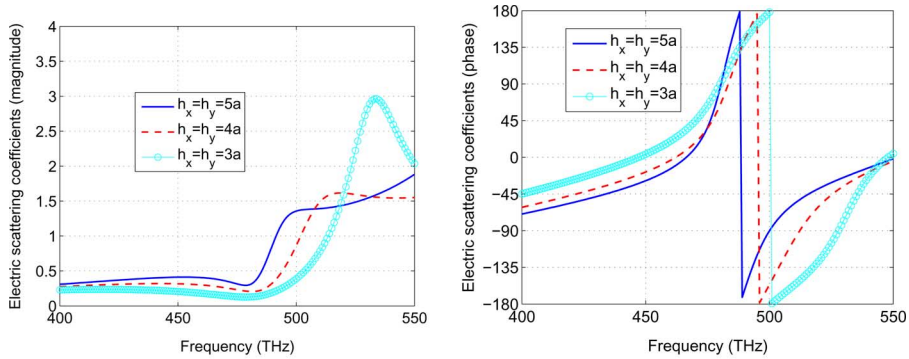

Fig. 13. Electric scattering coefficients behavior for a periodic array of GaP nanospheres with three layers in the direction of propagation, and $\epsilon_r = 12.25$, $a = 85$ nm, $d = 2.23a$ versus different unit cell sizes in the transverse direction (only the middle layer's scattering coefficient is plotted). (a) Magnitude. (b) Phase.

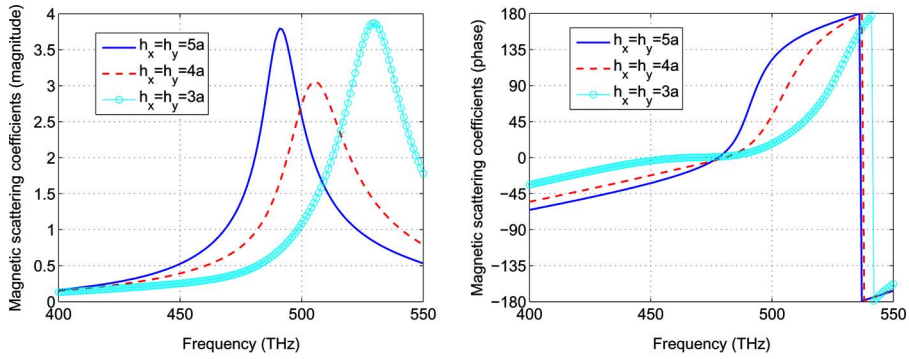

Fig. 14. Magnetic scattering coefficients behavior for a periodic array of GaP nanospheres with three layers in the direction of propagation, and $\epsilon_r = 12.25$, $a = 85$ nm, $d = 2.23a$ versus different unit cell sizes in the transverse direction (only the middle layer's scattering coefficient is plotted). (a) Magnitude. (b) Phase.

It can be deduced that, the backward phenomena are created because of the high coupling between the nanospheres. To verify this further, the performance of the scattered coefficients decrease the coupling (enlarging the unit cell sizes) is also analyzed. Figs. 13 and 14 present the electric and magnetic scattering coefficients for a three-layer array of GaP nanospheres with $a = 85$ nm, $d/a = 2.23$, and $h_x = h_y$. As observed, for $h_x/a = h_y/a \geq 4$, the electric scattering coefficients do not provide the resonant behavior at the resonance of magnetic scattering coefficients. Also, Figs. 13(b) and 14(b) exhibit that by increasing the transverse distance, the phases of scattering coefficients do not show the negative slope performances after the resonance, even for $h_x/a = h_y/a = 3$. These signify that, to provide the backward wave phenomena, the coupling in the transverse direction should be high enough. Figs. 15 and 16 illustrate the dependence of scattering coefficients on d, given h_x and h_y. The magnitude of electric and magnetic scattering coefficients show the resonance performance around the same frequency spectrum for all the cases presented in Figs. 15(a) and 16(a); however, the negative slope of the phase switches to positive slope for $d/a = 4$.

It is interesting to note that by decreasing the periodicity in the transverse direction (h_x and h_y), increasing the coupling, the electric resonance is moved back over the frequency (and appears in the spectrum of interest) where the magnetic resonance is slightly moved forward, where for an optimal design, both modes occur around the same frequency band. Making the spheres closer in the transverse plane, one can envision increasing the capacitances between the dielectric spheres. This has a positive effect for electric mode creation while slightly perturbs the magnetic mode development. By increasing the periodicity in the longitudinal direction (d), both electric and magnetic resonances are moved in the same direction toward the lower frequency (for large d, the brag modes play important roles in the performance).

To better demonstrate the progression of backward wave behavior, we also explore the dispersion diagram for an infinite array of spheres in the following section.

IV. Dispersion Diagram

Dispersion diagram of a periodic configuration can provide significant physical features. In this section, the dispersion performance of the 3-D array of dielectric nanospheres is characterized. The array is considered to be infinite in all directions ($L_x = L_y = \infty, l_z = 0, \pm 1, \ldots, \pm\infty$). We take the z-axis to be the array axis. It is assumed that the array can support a plane

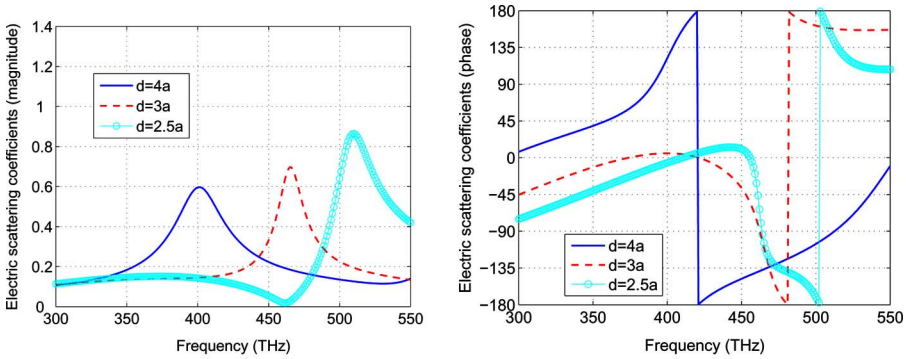

(a) (b)

Fig. 15. Performance of electric scattering coefficients for a periodic array of GaP nanospheres with three layers in the direction of propagation, and $\epsilon_r = 12.25$, $a = 85\,\mathrm{nm}, h_x = h_y = 2.23a$ versus different unit cell sizes in the propagation direction (only the middle layer's scattering coefficient is depicted). (a) Magnitude. (b) Phase.

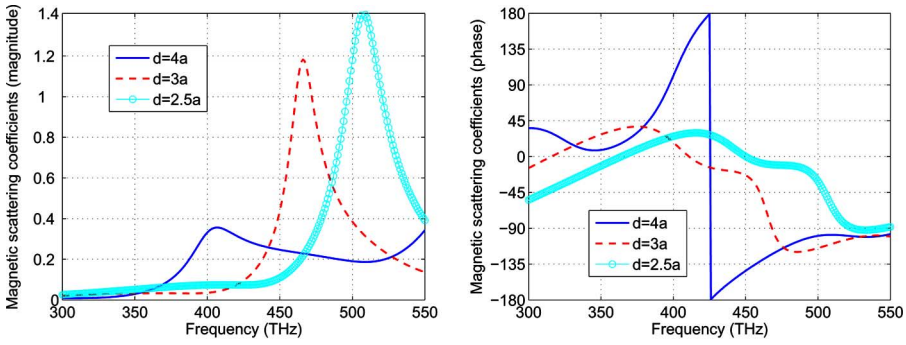

(a) (b)

Fig. 16. Performance of magnetic scattering coefficients for a periodic array of GaP nanospheres with three layers in the direction of propagation, and $\epsilon_r = 12.25$, $a = 85\,\mathrm{nm}, h_x = h_y = 2.23a$ versus different unit cell sizes in the propagation direction (only the middle layer's scattering coefficient is depicted). (a) Magnitude. (b) Phase.

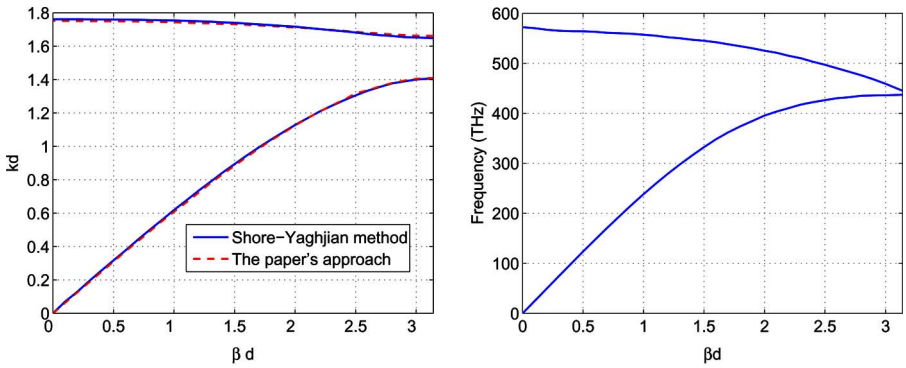

(a) (b)

Fig. 17. Dispersion diagrams characteristics for the 3-D array of nanospheres. (a) Comparison between our approach and the technique introduced in [29] for an array of nanospheres with $\epsilon_r = 20, a = 0.5\,\mathrm{cm}$, and cubical unit cell with $a/d = 0.45$. A very good match is achieved. (b) Engineered dispersion diagram for an array of GaP nanospheres with $\epsilon_r = 12.25$, $a = 85\,\mathrm{nm}$, and unit cell size with $d/a = 2.23$ and $h_x = h_y = 2.1a$. The second branch shows the backward wave behavior.

wave with the propagation vector $\boldsymbol{\beta}$, where

$$\boldsymbol{\beta} = \beta_x \hat{x} + \beta_y \hat{y} + \beta \hat{z}. \tag{18}$$

To obtain the dispersion diagram, the eigenvalue problem is solved, namely we force the incident expansion coefficients to be zero ($A^{ip}_{mn} = B^{ip}_{mn} = 0$). Inasmuch we have a uniform array of infinite dielectric nanospheres, the electric and magnetic scattering coefficients due to a plane wave with the propagation vector β are identical except for a phase shift in the direction of propagation

$$(A/B)^{sp}_{mn} = (A/B)^{sq}_{mn} e^{-j\boldsymbol{\beta}.\mathbf{d}_{\mathbf{qp}}}. \tag{19}$$

Substituting (19) in (11), we end up with

$$A_{mn}^{s0} = \varsigma_n(a)\left(\sum_{\substack{q\\ q\neq 0}}\sum_{\nu=1}^{\infty}\sum_{\mu=-\nu}^{\nu} e^{-j\boldsymbol{\beta}.\mathbf{d_{0q}}}\left[A_{mn}^{\mu\nu}(d_{pq},\theta_{pq},\phi_{pq})A_{\mu\nu}^{s0} + B_{mn}^{\mu\nu}(d_{pq},\theta_{pq},\phi_{pq})B_{\mu\nu}^{s0}\right]\right) \tag{20a}$$

$$B_{mn}^{s0} = \xi_n(a)\left(\sum_{\substack{q\\ q\neq 0}}\sum_{\nu=1}^{\infty}\sum_{\mu=-\nu}^{\nu} e^{-j\boldsymbol{\beta}.\mathbf{d_{0q}}}\left[A_{mn}^{\mu\nu}(d_{pq},\theta_{pq},\phi_{pq})B_{\mu\nu}^{s0} + B_{mn}^{\mu\nu}(d_{pq},\theta_{pq},\phi_{pq})A_{\mu\nu}^{s0}\right]\right) \tag{20b}$$

The desired dispersion equation is then achieved resolving the earlier system of equations for A_{mn}^{s0} and B_{mn}^{s0}. Notice that (20) is exact and no approximation is taken into the account. Moreover, the derived equations are general, and the dispersion performance for both normal and oblique incidence waves can be accomplished.

Now, if the nanospheres are sufficiently small or the frequency is such that pairs of crossed electric and magnetic dipoles are enough to model the sphere, the earlier linear system can be simplified further. For the special case of end-fire incidence

$$(A/B)_{11}^{s0} = (\varsigma_1(a)/\xi_1(a))\sum_{\substack{q\\ q\neq 0}} e^{-j\beta\hat{z}.\mathbf{d_{0q}}}\left[(A/B)_{11}^{s0} \times A_{11}^{11}(d_{0q},\theta_{0q},\phi_{0q}) + (B/A)_{11}^{s0}B_{11}^{11}(d_{0q},\theta_{0q},\phi_{0q})\right] \tag{21a}$$

One can numerically solve (21) for βd, given values of k using, for instance, a secant search procedure. It is worth highlighting that, the series in (21) are slowly convergent and an excessive number of terms is required to acquire the desired accuracy. Hence, to ease the computer programming, rapidly convergent solutions are applied [27], [29].

To evaluate the accuracy of our approach, we compare the dispersion diagram obtained by using the approach of our paper and the technique discussed in [29]. For a 3-D array of high dielectric spheres with $\epsilon_r = 20$, $a = 85$ nm and cubical unit cell of $a/d = 0.45$, the diagrams in Fig. 17(a) reveal a very good agreement

Fig. 17(b) displays the dispersion diagram for the array of dielectric GaP nanospheres with $\epsilon_r = 12.25$ and radius of $a = 85$ nm having the unit cell size of $h_x = h_y = 2.1a$ and $d/a = 2.23$. As it is shown, a negative slope backward wave with relatively large bandwidth is established. This occurs in the spectrum where the scattering coefficients show the resonance behavior (Figs. 11 and 12).

Basically, bringing the spheres closer to each other will increase the electric coupling between the spheres where it can be combined with the magnetic-mode performance of spheres above their magnetic resonances, offering a hybrid mode with backward wave phenomenon.

V. Summary

In this paper, theoretical investigation of all dielectric nanometamaterials is addressed. A FW spherical modal analysis is applied to express the optical fields in terms of the electric and magnetic dipole modes and the higher order terms. Imposing the boundary conditions at the surface of each nanosphere, using the translational addition theorem for vector spherical wave functions, required equations to determine the scattered coefficients are obtained. We show that if the nanospheres are small enough or the frequency is such that the magnitude of higher order modes are negligible compared to dipole modes, it is enough to model each particle with only dipole spherical waves.

The concept of electric and magnetic dipole modes generation for metapatterned structure development is presented. We demonstrate that by bringing the dielectric spheres close to each other, the electric coupling between them are increased such that both electric and magnetic resonances can be achieved around the same frequency region. After the resonances, the phases of the scattering coefficients show the negative slope behavior. Dispersion diagram characteristic for an array of highly coupled spheres is investigated and the backward wave phenomenon is achieved.

A capable modeling technique by utilizing RLC circuit theory for characterizing the scattering coefficients is presented. Following the same analogy, the couplings between spheres are also described in a type of circuit realization. Computational results verify the accuracy of circuit models in predicting the performance of nanostructures.

The success of this study may open new paradigms for high-performance electric and magnetic dipole mode creations in optics, using nonmagnetic particles.

References

[1] N. Engheta and R. W. Ziolkowski, *Metamaterials: Physics and Engineering Explorations*. New York: Wiley, 2006.

[2] C. Caloz and T. Itoh, *Electromagnetic Metamaterials: Transmission Line Theory and Microwave Applications*. New York: Wiley, 2006.

[3] G. V. Eleftheriades and K. G. Balmain, *Negative-Refraction Metamaterials*. New York: Wiley, 2005.

[4] A. Ahmadi and H. Mosallaei, "Physical configuration and performance modeling of all-dielectric metamaterials," *Phys. Rev. B*, vol. 77, 045104, 2008.

[5] S. Ghadarghadr and H. Mosallaei, "Dispersion diagram characteristics of periodic array of dielectric and magnetic materials based spheres," *IEEE Trans. Antennas Propag.*, vol. 57, no. 1, pp. 149–160, Jan. 2009.

[6] C. L. Holloway, E. F. Kuester, J. Baker-Jarvis, and P. Kabos, "A double negative (D N G) composite medium composed of magnetodielectric spherical particles embedded in a matrix," *IEEE Trans. Antennas Propag.*, vol. 51, no. 10, pp. 2596–2603, Oct. 2003.

[7] L. Lewin, "The electrical constants of a material loaded with spherical particles," *Proc. Inst. Electr. Eng.*, vol. 94, pp. 65–68, 1947.

[8] O. G. Vendik and M. S. Gashinova, "Artificial double negative (DNG) media composed of two different dielectric sphere lattices embedded in a dielectric matrix," in *Proc. 34th Eur. Microw. Conf.,* 2004, Amsterdam, The Netherlands, pp. 1209–1212.

[9] Y. Luo, S. K. Lee, H. Hofmeister, M. Steinhart, and U. Gosele, "Pt nanoshell tubes by template wetting," *Nano Lett.*, vol. 4, no. 1, pp. 143–147, 2004.

[10] S. Dey and R. Mittra, "A locally conformal finite-difference time-domain (fdtd) algorithm for modeling three-dimensional perfectly conducting objects," *IEEE Lett. Microw. Guided Wave*, vol. 7, no. 9, pp. 273–275, Sep. 1997.
[11] C. Oubre and P. Nordlander, "Optical properties of metallodielctric nanostructure calculated using the finite difference time domain method," *J. Phys. Chem. B*, vol. 108, pp. 17740–17747, 2004.
[12] K. L. Shlager and J. B. Schneider, "A selective survey of the finite-difference time-domain literature," *IEEE Mag. Antenna Propag.*, vol. 37, no. 4, pp. 39–57, Aug. 1995.
[13] S. Zou and G. C. Schatz, "Narrow plasmonic/photonic extinction and scattering line shapes for one and two dimensional silver nanoparticle arrays," *J. Phys. Chem.*, vol. 121, no. 24, pp. 12 606–12 612, 2004.
[14] J. L. Volakis, A. Chatterjee, and L. C. Kempel, *Finite Element Method for Electromagnetics*. New York: IEEE Press, 1998.
[15] A. Taflove and S. C. Hagness, *Computational Electromagnetics The Finite-Difference Time-Domain Method*, 3rd ed. Norwood, MA: Artech House, 2005.
[16] P. J. Flatau, "Fast solvers of one dimensional light scattering in the discrete dipole approximation," *Opt. Exp.*, vol. 12, no. 14, pp. 3149–3155, 2004.
[17] M. Alam and Y. Massoud, "A closed-form analytical model for single nanoshells," *IEEE Trans. Nanotechnol.*, vol. 5, no. 3, pp. 265–272, May 2006.
[18] M. Alam and Y. Massoud, "RLC ladder model for scattering in single metallic nanoparticles," *IEEE Trans. Nanotechnol.*, vol. 5, no. 5, pp. 491–498, Sep. 2006.
[19] G. W. Hanson and P. Smith, "Modeling the optical interaction between a carbon nanotube and a plasmon resonant sphere," *IEEE Trans. Antennas Propag.*, vol. 55, no. 11, pp. 3063–3069, Nov. 2007.
[20] J. D. Jackson, *Classical Electrodynamics*. New York: Wiley, 1999.
[21] V. Rumsey, "A short way of solving advanced problems in electromagnetic fields and other linear systems," *IEEE Trans. Antennas Propag.*, vol. AP-11, no. 1, pp. 73–86, Jan. 1963.
[22] O. R. Cruzan, "Translational addition theorems for spherical vector wave," *Q. Appl. Math.*, vol. 20, pp. 33–40, 1962.
[23] A.-K. Hamid, I. R. Ciric, and M. Hamid, "Electromagnetic scattering by an arbitrary configuration of dielectric spheres," *Can. J. Phys.*, vol. 68, pp. 1419–1428, 1990.
[24] J. A. Stratton, *Electromagnetic Theory*. New York: McGraw-Hill, 1941.
[25] H. Thal, Jr., "Exact circuit analysis of spherical waves," *IEEE Trans. Antennas Propag.*, vol. 26, no. 2, pp. 282–287, 1978.
[26] M. Abramowitz and I. A. Stegun, *Handbook of Mathematical Functions*. New York: Dover, 1972.
[27] I. S. Gradshteyn and I. M. Ryzhik, *Table of Integrals, Series and Products*. Boston, MA: Academic, 1994.
[28] R. A. Shore and A. D. Yaghjian, "Traveling waves on two- and three-dimensional periodic arrays of lossless acoustic monopoles, electric dipoles, and magnetodielectric spheres," Air Force Research Lab. Hanscom, MA, in house report, 2006.
[29] R. A. Shore and A. D. Yaghjian, "Traveling waves on two- and three-dimensional periodic arrays of lossless scatterers," *Radio Sci. RS6S21*, vol. 42, 2007. (Doi:10.1029/2007RS003647).

Shabnam Ghadarghadr (S'05) received the B.Sc. degree (with highest honors) from Shiraz University, Shiraz, Iran, in 2005. She is currently working toward the Ph.D. degree in the Department of Electrical and Computer Engineering, Northeastern University, Boston, MA.

Since 2006, she has been a Graduate Research/Teaching Assistant in the Advanced Electromagnetics (EM) and Optics Devices Laboratory, Northeastern University. Her current research interests include theoretical electromagnetic, theory and applications of metamaterials, nanoelectromagnetics, optical antennas, waves interaction in complex media, and photonic bandgap structures.

Hossein Mosallaei (S'98–M'02–SM'02) received the B.Sc. and M.Sc. degrees in electrical engineering from Shiraz University, Shiraz, Iran, in 1991 and 1999, respectively, and the Ph.D. degree in electrical engineering from the University of California, Los Angeles (UCLA), in 2001. He is currently an Assistant Professor of electrical and computer engineering in the Electrical and Computer Engineering Department Northeastern University, Boston, MA.

From 2002 to 2005, he was an Assistant Research Scientist in The Electrical Engineering and Computer Science (EECS) Department, University of Michigan.

Dr. Mosallaei was the Vice Chair of the IEEE Michigan Trident Chapter (Antennas and Propagation, Microwave Theory and Techniques, Electron Devices) in 2005. He is a full member of the Union of Radio Science International (URSI), and a member of the American Association for the Advancement of Science. He is listed in Who's Who in Science and Engineering, Who's Who in America, and Who's Who in the World. He has organized several special sessions in various IEEE conferences. He has been also a plenary session speaker in many national and international symposia. He is the holder of one US patent. He is the author or coauthor of more than 100 technical journal articles and conference papers.

He was the recipient of Student Prize Paper Awards in Antennas and Propagation Society (AP-S) 2000, 2001, 2003, and 2005 with his student, URSI Young Scientist Award in 2001, and Raj Mittra Travel Grant (RMTG) Award in 2002. His research interests include Applied Electromagnetics and Micro/Nanoscale RF-THz Devices.